Friction and wear of human hair fibres

Journal Item

Friction and wear of human hair fibres

James Bowen,[1*] Simon A Johnson,[2] Andrew R Avery,[2] Michael J Adams[3]

[1] Department of Engineering and Innovation, The Open University, Walton Hall, Milton Keynes, MK7 6AA, UK

[2] Unilever R&D Port Sunlight, Quarry Road East, Bebington, Wirral, CH63 3JW, UK

[3] School of Chemical Engineering, The University of Birmingham, Edgbaston, Birmingham, B15 2TT, UK

* To whom correspondence should be addressed

Email: james.bowen@open.ac.uk

Telephone: + 44 (0) 1908 655 614

Keywords

Fibre, friction, hair, interferometry, SEM, tribology, wear

Abstract

An experimental study of the tribological properties of hair fibres is reported, and the effect of surface treatment on the evolution of friction and wear during sliding. Specifically, orthogonally crossed fibre/fibre contacts under a compressive normal load over a series of 10,000 cycle studies are investigated. Reciprocating sliding at a velocity of 0.4 mm/s, over a track length of 0.8 mm, was performed at 18^{o}C and 40-50% relative humidity. Hair fibres retaining their natural sebum were studied, as well as those stripped of their sebum via hexane cleaning, and hair fibres conditioned using a commercially available product. Surface topography modifications resulting from wear were imaged using scanning electron microscopy and quantified using white light interferometry. Hair fibres that presented sebum or conditioned product at the fibre/fibre junction exhibited initial coefficients of friction at least 25% lower than those that were cleaned with hexane. Coefficients of friction were observed to depend on the directionality of sliding for hexane cleaned hair fibres after sufficient wear cycles that cuticle lifting was present, typically on the order 1,000 cycles. Cuticle flattening was observed for fibre/fibre junctions exposed to 10 mN compressive normal loads, whereas loads of 100 mN introduced substantial cuticle wear and fibre damage.

1. Introduction

Hair is a protein-based biomaterial that grows in filament-like structures from follicles beneath the surface of the skin. In humans there are different types of hair, each of which provide a particular function, including heat retention and tactile sensation. The evolution, structure and function of human hair is of great interest to anatomists and anthropologists [1], and the use of hair for social and cultural functions is well established. The importance of hair style, feel, and appearance to the owner and to those with whom the owner interacts is beyond doubt in today's well-groomed society. There have been a range of scientific studies regarding the structure of hair [2-3], the causes of hair damage [4-5], and the physicochemical properties of the hair cuticle surface [6-7]. Furthermore, the mechanical properties of individual fibres have been a topic of interest for a number of researchers [8-12]. Particular attention has been given to the use of atomic force microscopy (AFM) for studying friction and conditioners applied to single hair fibres [13-22].

Tribology is a relatively new field of scientific study, although the first investigations into friction can be traced back to pioneers including Da Vinci, Amontons, and Reynolds [23]. As the ability to investigate micro- and nanoscale phenomena has improved, so has our understanding of friction and lubrication at surfaces and interfaces. The use of lubricants to treat and protect hair fibres has long been a fundamental feature of hair care products, providing a tribological safety barrier to wear damage. For example, the act of combing hair can generate compressive forces between adjacent fibres, which could lead to wear damage. Indeed, the formation of split ends has been related to the frictional forces generated during the combing process [4].The relative orientation and number of repeat strokes of contacting hair fibres as they slide across one another will have an influence on the stresses generated and the wear damage that results.

The hair fibre presents a topographically interesting and complex substrate, with an anisotropic directional dependence, due to the growth mechanism of the hair cuticle, and the structure which forms as a result. Adams *et al*. previously demonstrated that differential friction effects observed with keratin fibres were due to the asymmetry presented by the cuticular structure of the fibre outer surface [24]. Building on this work, Mizuno *et al*. reported that the friction coefficient of native hair was relatively insensitive to the angle between crossed fibres, and that directional effects were not observed until cuticle lifting and serration were present [25].

The aim of this work is to quantify the frictional properties of fibre/fibre contacts under compressive normal load, with applied lateral sliding in both directions along a hair fibre. Virgin hair fibres will be tested for their tribological properties and propensity to wear, as will fibres stripped of their native sebum, which is hypothesized to act as a natural lubricant and protectant. Moreover, fibres that have been conditioned using a commercially available product will be tested as a comparison. The extent of any wear damage will be assessed via topographical analysis using white light interferometry (WLI). A nanotribometer is employed for these measurements because of the relatively large compressive normal loads which can be generated, typically in the range 10^{-2} to 1 N. This greatly exceeds the maximum normal load which can be applied using AFM operating high spring constant cantilevers, which is typically 10^{-6} to 10^{-5} N.

2. Methods

2.1 Hair fibre immobilisation. Hair fibres were immobilized onto 25 mm diameter aluminium scanning electron microscopy (SEM) stubs using a thin film of cyanoacrylate adhesive (Araldite, UK). Briefly, each hair fibre was held under slight tension above the adhesive-coated stub, which was then raised into contact with the hair fibre using a laboratory jack (Fisher Scientific, UK). After the adhesive had set and dried, the tension was removed from the hair fibre, followed by trimming the hair fibre length to match the stub diameter. No defects were observed at this stage, and the hair fibre was ensured to have retained strong adhesion to the aluminium stub. Attempting to trim the hair fibre without removing the tension led to failure of the fibre/adhesive bond. A schematic of the immobilisation process for the Test hair fibre is shown in **Fig. 1**. A similar procedure was used to adhere the Probe hair fibre to the Nanotribometer cantilever.

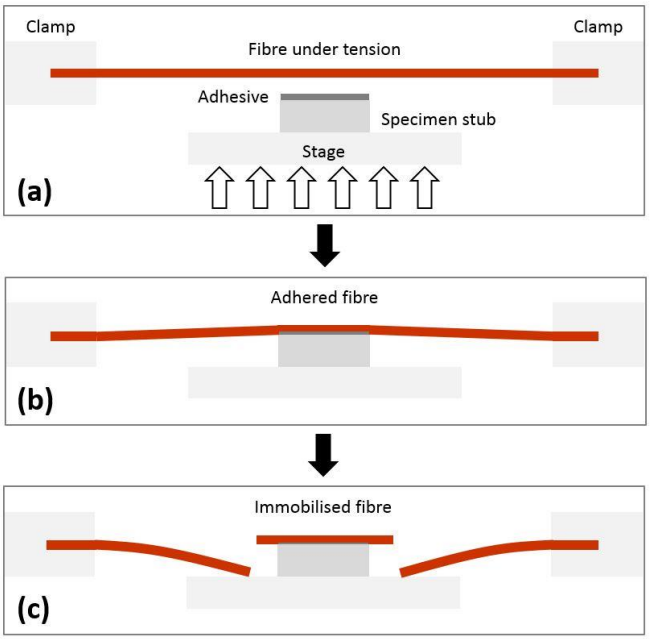

Figure 1. Immobilisation of hair fibres. (a) Adhesive-coated stub raised into contact with hair fibre held under tension; (b) adhesive allowed to dry; (c) hair fibre trimmed after tension is removed.

2.2 Topographical analysis. Three-dimensional hair fibre topographies were acquired using a white light Interferometer (KLA Tencor, USA). Images were acquired using a 50X lens over an area with dimensions 86 µm x 64 µm. Image analysis was performed using Scanning Probe Image Processor software (Image Metrology, Denmark). Prior to roughness analysis, the cylindrical curvature of the hair fibre was subtracted by fitting a 2nd order polynomial to the data. SEM images of hair fibre topography were acquired using a TM3000 Tabletop Microscope (Hitachi, UK). Due to the anisotropic morphology of the hair fibre surface, care was taken to denote the directionality of each Test hair fibre. With reference to **Fig. 2**, 'With cuticle' is the sliding direction which would travel along the cuticle until reaching a height decrease at the edge between two overlapping cells; this corresponds to the 'root-to-tip' direction. 'Against cuticle' is the sliding direction which would travel along the cuticle until reaching a height increase at the edge between two overlapping cells; this corresponds to the 'tip-to-root' direction.

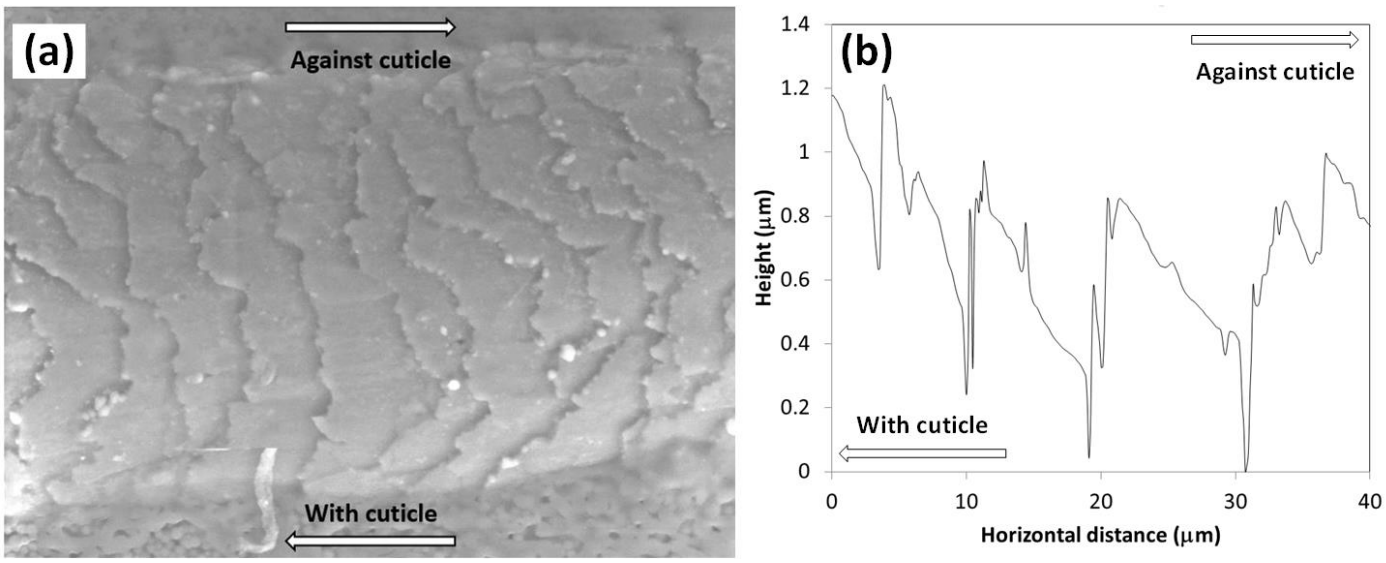

Figure 2. Virgin hair fibre structure showing 'With cuticle' and 'Against cuticle' directions. (a) SEM image, image dimensions 90 μm x 67 μm; (b) line profile acquired using white light interferometry.

2.3 Hair fibre treatment. Hair fibres were treated in three different ways: (i) virgin, i.e. used as received (International Hair Importers, USA); (ii) hexane cleaned, to remove native sebum; (iii) conditioned. Hexane cleaned hair fibres were completely immersed in a shallow bath of hexane (analytical grade, Fisher Scientific, UK) for 5 min, before being removed and allowed to dry under ambient conditions (18 ^{o}C, 40-50% relative humidity). Hexane cleaning was performed prior to immobilization, otherwise the hexane would dissolve the cyanoacrylate adhesive. Conditioning was performed on immobilised hair fibres, which had previously been hexane cleaned, via application of approximately 0.2 g conditioner (Dove, Unilever, UK) for 1 min; it was applied using a cotton bud. This was followed by rinsing with water (HPLC grade, Sigma-Aldrich, UK) and gentle sweeping using a water-soaked cotton bud for 1 min. Contact was made with the hair fibre only whilst sweeping in the 'With cuticle' direction, to prevent inadvertent cuticle damage or lifting. The same procedure was used to treat both the Probe and Test hair fibres.

2.4 Tribological testing. Tribological measurements were performed using a NTR1 Nanotribometer (CSM Instruments, Switzerland) operating under ambient conditions of 18 ^{o}C and 40-50% relative humidity. A schematic is shown in **Fig. 3**. Hair fibres were oriented such that the 'Against cuticle' direction matched the initial sliding direction. The Probe hair fibre was held at an angle of 90^{o} to the Test hair fibre. Tests were performed at compressive normal loads of 10 and 100 mN. Upon the target normal load being achieved, a reciprocating motion was applied to the Test hair fibre, over a 0.8 mm track length at a sliding velocity of 0.4 mm/s. The NTR1 operated in closed loop mode, such that the normal load was maintained to within ± 1% of the set point value throughout the duration of the test. The target number of reciprocating cycles was 10^4, which corresponded to 10^4 passes in each direction; this corresponded to a test duration of approximately 11 hours. Tangential and normal loads were recorded at a data capture rate of 10 Hz during testing. The Test hair fibre was carefully removed from the Nanotribometer and assessed for wear post-test using WLI.

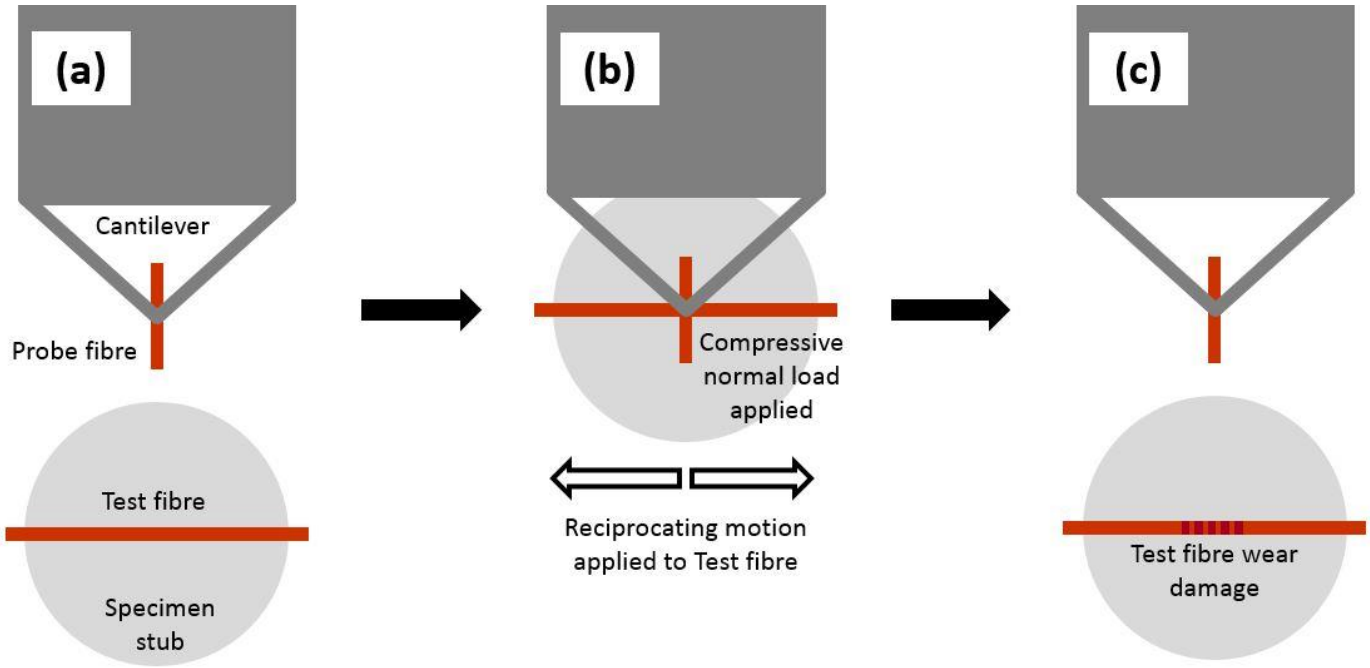

Figure 3. Tribological testing. (a) Probe hair fibre oriented at an angle of 90° to the Test hair fibre; (b) compressive normal load applied and maintained during reciprocating sliding; (c) damage to Test hair fibre assessed upon completion of the test.

3. Results

3.1 Virgin hair fibres

Fig. 4(a) shows the surface topography of a virgin hair fibre acquired using WLI. Similar to **Fig. 2**, the overlapping cuticle structure can be seen as a series of angled surfaces approximately 10 µm in length. The cuticle structure of human hair is analogous to a series of stacked paper cups. **Fig. 4(a)** is truncated in the y-direction due to the curvature of the fibre, which means that the intensity of reflected light reaching the Interferometer lens decreases rapidly away from the central, upper section of the cylindrical fibre. The mean cuticle height of a virgin hair fibre is 369 ± 33 nm. The average roughness, S_a, of **Fig. 4(a)** is 195 nm, whilst the peak-to-valley height, S_y, is 4.38 µm. **Fig. 4(b)** shows the histogram of pixel heights for the image in **Fig. 4(a)**. The skewness and kurtosis for this distribution are S_{sk} =1.00 and S_{ku} =10.2 respectively. Void pixels in Fig. 4(a), shown in white, are due to the high local curvature of the surface at that pixel, typically at a cuticle edge. The light intensity reflected into the lens and detector at this position was insufficient to trigger a recording above the background noise level of the detector.

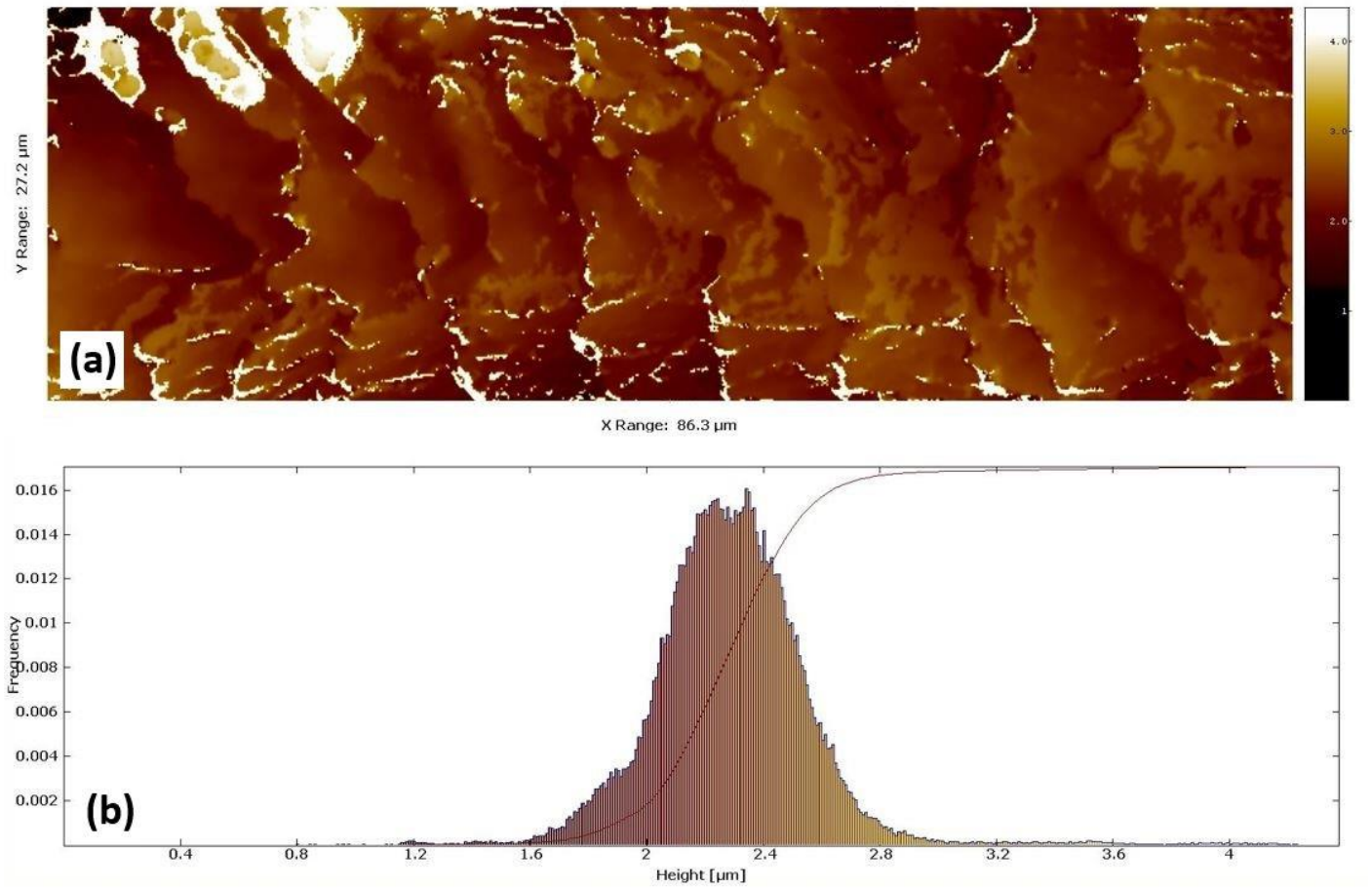

Figure 4. Surface topography of virgin hair fibre. (a) Structure obtained using white light interferometry, void pixels are shown in white; (b) histogram of pixel heights for image shown in (a).

3.2 Virgin hair fibres, $F_N = 100$ mN

Fig. 5(a) shows the evolution of the tangential load as a function of cycle number for two orthogonally crossed virgin hair fibres, sliding relative to each other whilst a compressive normal load of 100 mN is maintained. Within the first 5 cycles the tangential load reaches a similar value for both the 'Against cuticle' and 'With cuticle' sliding directions, approximately 5-7 mN. After approximately 10^2 cycles the tangential load increases towards 8-10 mN, and remains in that load range between 10^3-10^4 cycles. **Fig. 5(b)** shows a wear track along the highest section of the cylindrical hair fibre, in which region the cuticle has been damaged. The width of the wear track is approximately 8 µm, which is consistent with the radius of the contact region, assuming Hertz theory applies [26]. The contact mechanics calculation is given in Appendix A1, where the Young's modulus of the hair fibre cuticle is assumed to be 8 GPa [27] and the Poisson's ratio is assumed to be 0.38 [28-29]. The hair fibre region shown in **Fig. 5(b)** exhibits the following statistical parameters: $S_a = 339$ nm, $S_y = 3.37$ µm, $S_{sk} = -0.27$, and $S_{ku} = 2.59$.

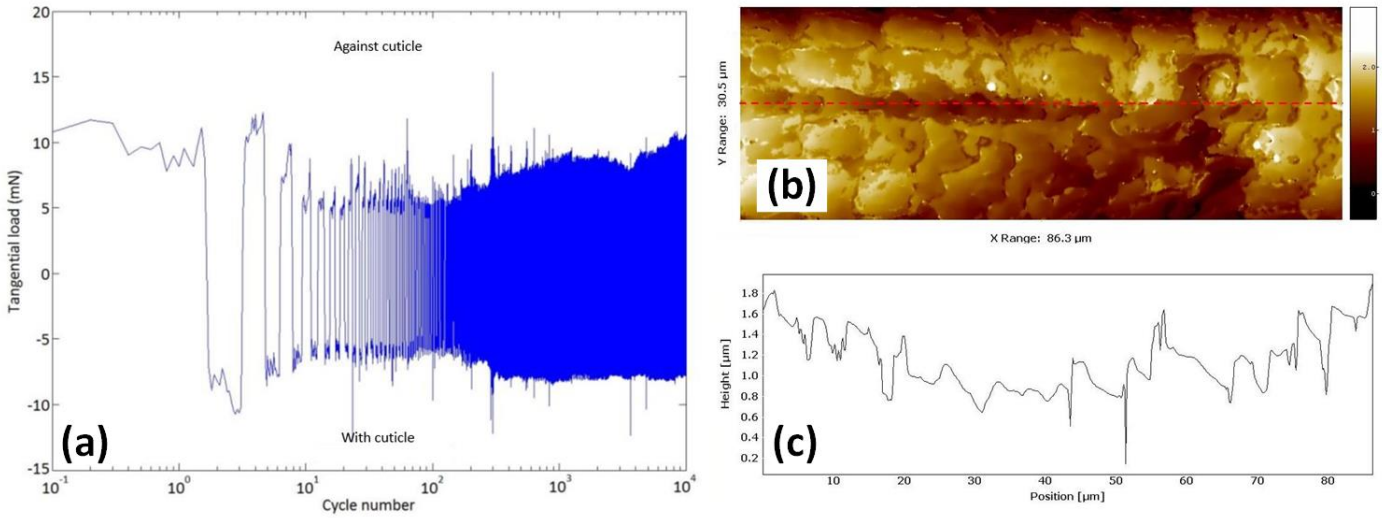

Figure 5. Tribological testing results for virgin hair fibres, $F_N = 100$ mN. (a) Tangential load as a function of cycle number; (b) topography and wear track after 10^4 cycles, acquired using white light interferometry; (c) line profile across wear track, indicated by dashed line in (b).

3.3 Hexane cleaned hair fibres, $F_N = 10$ mN

Fig. 6(a) shows the evolution of the tangential load as a function of cycle number for two orthogonally crossed hexane cleaned hair fibres, sliding relative to each other whilst a compressive normal load of 10 mN is maintained. During the first 10^2 cycles the tangential load in both the 'Against cuticle' and 'With cuticle' sliding directions is within the range 5-8 mN. Between 10^2-10^4 cycles the tangential load increases gradually towards 12-15 mN in the 'With cuticle' direction. In contrast, the tangential load increases to 20 mN in the 'Against cuticle' direction. Hence, a differential friction effect is exhibited once the cuticles start to become damaged. **Fig. 6(b)** shows that substantial wear has occurred along the sliding track, the cuticle is no longer visible, and wear debris is present throughout the image. The hair fibre region shown in **Fig. 6(b)** exhibits the following statistical parameters: $S_a = 853$ nm, $S_y = 7.16$ µm, $S_{sk} =$ -0.45, and $S_{ku} = 2.44$.

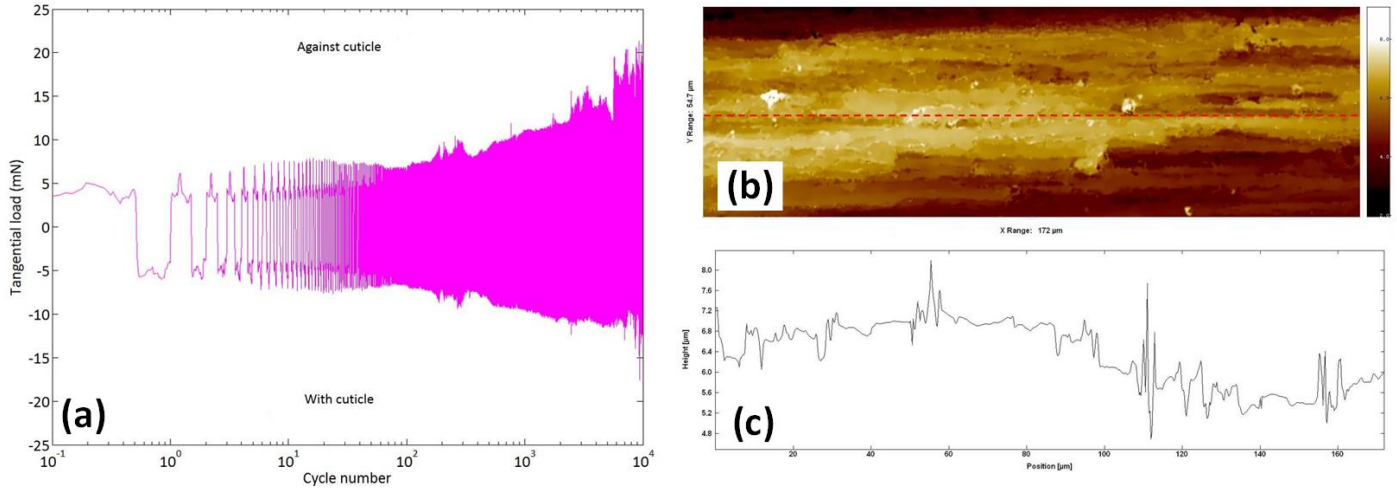

Figure 6. Tribological testing results for hexane cleaned hair fibres, $F_N = 10$ mN. (a) Tangential load as a function of cycle number; (b) topography and wear track after 10^4 cycles, acquired using white light interferometry; (c) line profile across wear track, indicated by dashed line in (b).

3.4 Hexane cleaned hair fibres, $F_N = 100$ mN

Fig. 7(a) shows the evolution of the tangential load as a function of cycle number for two orthogonally crossed hexane cleaned hair fibres, sliding relative to each other whilst a compressive normal load of 100 mN is maintained. During the first 30 cycles the tangential load in both the 'Against cuticle' and 'With cuticle' sliding directions is within the range 15-20 mN. Between 30-10^2 cycles the tangential load increases rapidly towards 40 mN in the 'With cuticle' direction and 35 mN in the 'Against cuticle' direction. Hence, a differential friction effect is exhibited from here on. Further increases in tangential load give rise to values of 100 mN in the 'With cuticle' direction and 90 mN in the 'Against cuticle' direction after 3,000 cycles, which are approximately maintained until 10^4 cycles. **Fig. 7(b)** shows that substantial wear has occurred along the sliding track, the cuticle is no longer visible, and a deep groove is present along the centre of what was previously a cylindrical fibre. The hair fibre region shown in **Fig. 7(b)** exhibits the following statistical parameters: $S_a = 844$ nm, $S_y = 9.39$ µm, $S_{sk} =$ -0.72, and $S_{ku} = 2.71$.

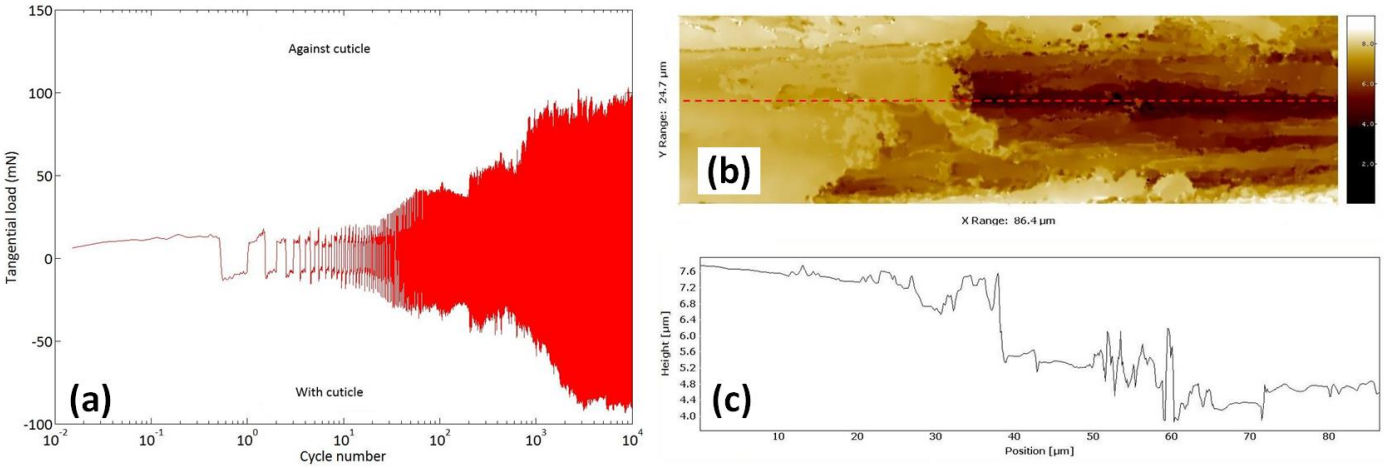

Figure 7. Tribological testing results for hexane cleaned hair fibres, $F_N = 100$ mN. (a) Tangential load as a function of cycle number; (b) topography and wear track after 10^4 cycles, acquired using white light interferometry; (c) line profile across wear track, indicated by dashed line in (b).

3.5 Conditioned hair fibres, $F_N = 10$ mN

Fig. 8(a) shows the evolution of the tangential load as a function of cycle number for two orthogonally crossed conditioned hair fibres, sliding relative to each other whilst a compressive normal load of 10 mN is maintained. During the first 20 cycles the tangential load in the 'Against cuticle' sliding direction decreases from 1 mN towards 0.5-0.6 mN, and remains within this range until approximately 10^2 cycles. The tangential load then increases rapidly to 0.7-0.8 mN and remains in that range until cycle 3,000, before increasing further towards 1.4 mN, when this test terminated. In the 'With cuticle' direction, the tangential load has an approximately constant value of 0.6-0.8 mN until 700 cycles. The tangential load then increases steadily with cycle number, reaching 1.4 mN at the cycle when this test terminated. **Fig. 8(b)** shows that substantial wear has not occurred along the sliding track, although the cuticle now appears flattened and stretched when compared to **Fig. 4(a)**. The hair fibre has sustained mechanical damage due to the compressive loading and lateral sliding, but this has occurred beneath the cuticle, rather than manifest as a delamination or partial fracture of the cuticle. The hair fibre region shown in **Fig. 8(b)** exhibits the following statistical parameters: $S_a = 457$ nm, $S_y = 3.15$ µm, $S_{sk} =$ -0.55, and $S_{ku} = 2.39$.

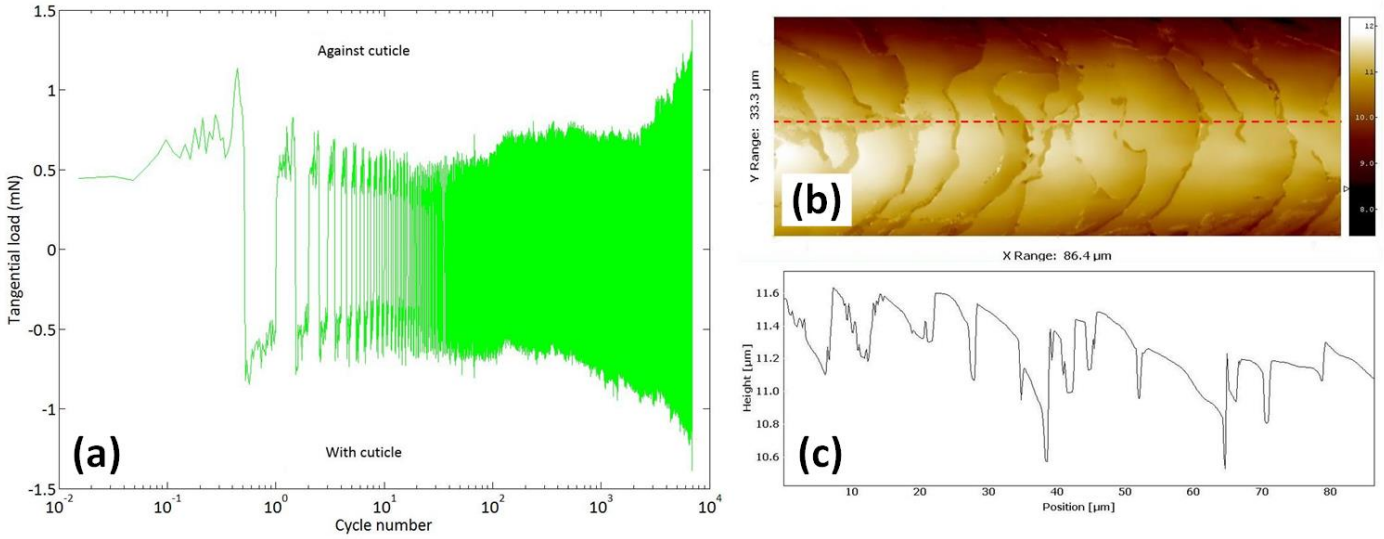

Figure 8. Tribological testing results for conditioned hair fibres, $F_N = 10$ mN. (a) Tangential load as a function of cycle number; (b) topography and wear track after 7x10^3 cycles, acquired using white light interferometry; (c) line profile across wear track, indicated by dashed line in (b).

3.6 Conditioned hair fibres, $F_N = 100$ mN

Fig. 9(a) shows the evolution of the tangential load as a function of cycle number for two orthogonally crossed conditioned hair fibres, sliding relative to each other whilst a compressive normal load of 100 mN is maintained. During the first 200 cycles the tangential load in both the 'Against cuticle' and 'With cuticle' sliding directions is within the range 1.0-1.5 mN. Between 200-5,000 cycles, the tangential load does not exceed 2 mN in either sliding direction. After 5,000 cycles the tangential load undergoes a rapid increase, with evidence of a differential friction effect. By cycle 10^4 the tangential load is in excess of 8 mN in the 'Against cuticle' direction and approximately 5 mN in the 'With cuticle' direction. **Fig. 9(b)** shows that substantial wear has occurred along the sliding track, the cuticle is no longer visible, and wear debris is present throughout the image. The hair fibre region shown in **Fig. 9(b)** exhibits the following statistical parameters: $S_a = 446$ nm, $S_y = 5.65$ µm, $S_{sk} =$ -0.19, and $S_{ku} = 3.50$.

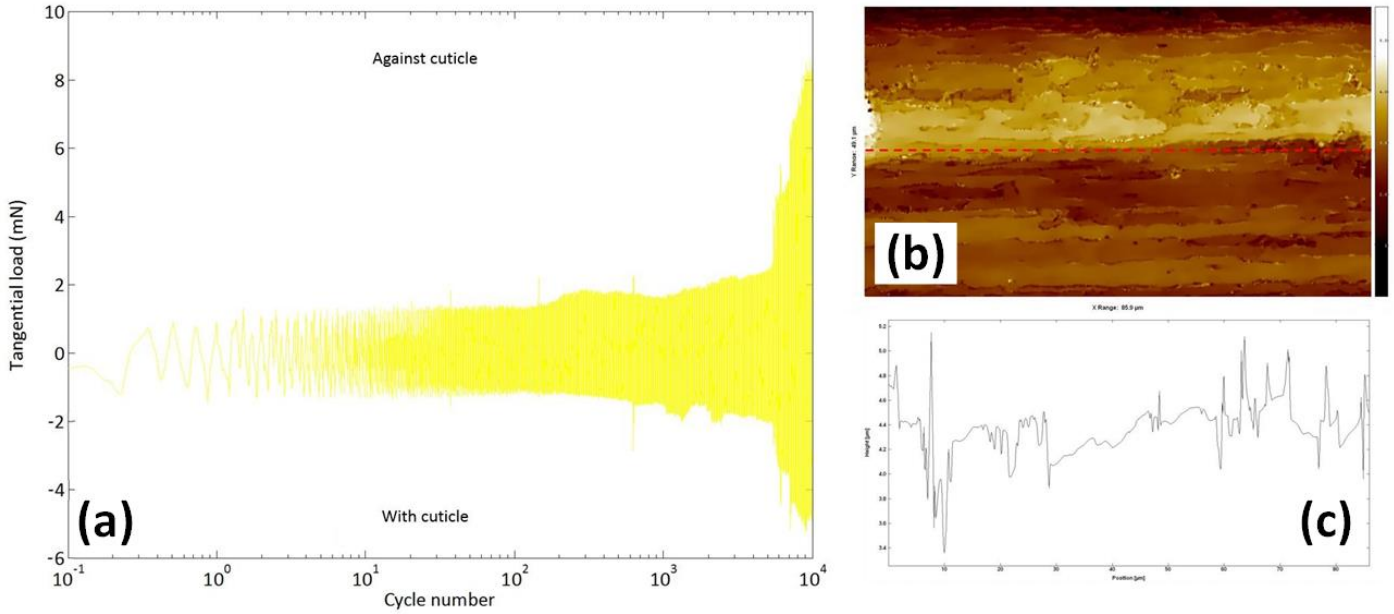

Figure 9. Tribological testing results for conditioned hair fibres, $F_N = 100$ mN. (a) Tangential load as a function of cycle number; (b) topography and wear track after 10^4 cycles, acquired using white light interferometry; (c) line profile across wear track, indicated by dashed line in (b).

4. Discussion

Fig. 10 shows the coefficient of friction as a function of the cycle number for each test performed. The plot demonstrates the evolution of frictional forces during each measurement, and aids comparison between tests. **Fig. 10** summarises the tribological testing data for all hair fibres investigated. For each test the measured tangential load has been normalized by the applied normal load, which yields a coefficient of friction, μ, which is calculated according to **Eq. 1**, where F_N is the normal load and F_T is the tangential load.

$$\mu = \frac{F_T}{F_N} \quad (1)$$

The tribological behaviour of virgin hair fibres at $F_N = 100$ mN (**Fig. 5**) sets a reasonable benchmark, whereby minimal damage was observed after 10^4 cycles, and the coefficient of friction never exceeds $\mu = 0.10$. Conditioned hair fibres at $F_N = 10$ mN (**Fig. 8**) displayed similar behaviour until 10^3 cycles, at which point the coefficient of friction increases to $\mu > 0.10$. Virgin hair fibres at $F_N = 100$ mN exhibited a small amount of cuticle wear, in-keeping with the diameter of the Hertzian contact spot which would be expected to form between the orthogonally crossed cylinders. Conditioned hair fibres at $F_N = 10$ mN exhibited no cuticle wear, but there was evidence of cuticle flattening, i.e. mechanical damage to the sub-cuticle hair fibre.

Conditioned hair fibres tested at $F_N = 100$ mN (**Fig. 9**) displayed coefficient of frictions $\mu < 0.02$ until cycle $5x10^3$, which are significantly lower than those exhibited by the virgin hair fibres at $F_N = 100$ mN or conditioned hair fibres at $F_N = 10$ mN. The exceptionally low value displayed by conditioned hair fibres at $F_N = 100$ mN was therefore surprising given the extent of visible damage in **Fig. 9(b)**. It is likely that the onset of damage corresponds to the sudden increase in friction around cycle $5x10^3$. Hence, although the conditioner imparts a lubricating layer onto the hair fibres, this was not sufficient to prevent hair fibre wear after sustained sliding at $F_N = 100$ mN. In contrast, the natural sebum presented by the virgin hair fibres did not promote coefficient of frictions as small as the conditioner could produce. However, it appears to have proven more effective at preventing wear and mechanical damage for tests performed at the same compressive normal load, $F_N = 100$ mN.

Hexane cleaning was found to increase the coefficient of friction substantially, particularly for tests performed at $F_N = 10$ mN (**Fig. 6**). Hexane cleaned hair fibres exhibited increases in the coefficient of friction during testing from cycle 50 onwards, with continually increasing values thereafter. The likely cause of this behaviour is the removal of native sebum from the hair fibre during the hexane immersion. Sebum composition varies with environmental conditions, but will usually consist of triglycerides, fatty acids, and long-chain hydrocarbons and hydrocarbon esters. Molecules of this type will induce a lubricating property to the hair fibre surface, which is consistent with the tribological properties measured for virgin hair fibres. Furthermore, these molecules are soluble in hexane, leading to their rapid removal during the cleaning/immersion procedure. Differential friction effects were only observed for hair fibres which had been hexane cleaned, and only after sufficient wear had occurred that the tangential load was significantly increased from its initial value. This is in-keeping with the result obtained by Mizuno *et al*. [25] whereby directional effects were not observed until cuticle lifting and serration were present on the fibre.

The tangential load can be recorded at a data capture rate suitable for detecting minor and major changes in the tribological behaviour. This provides useful information regarding the likely moment at which wear damage occurs. The possibility of constructing a custom apparatus to perform *in situ* monitoring of degradation, alongside measurement of the tangential load during sliding, is highly desirable. Such an apparatus could provide valuable information regarding the mechanisms via which wear begins and proceeds. As an alternative, the ability to pause a tribological test, inspect the region of the Test hair fibre under investigation, then continue with the test, could be of great value.

One limitation of this study is that a single-axis motion path is supplied to the Test hair fibre using the NTR1, and hence the Probe hair fibre is held stationary relative to this. A 0.8 mm region of the Test hair fibre undergoes tribological testing, whereas the region of the Probe hair fibre which is in contact during testing is perhaps less than 10 µm in diameter. It would be beneficial to construct an apparatus where the orthogonally crossed hair fibres are subjected to two-axis motion, whereby equal track lengths on both the Probe and Test hair fibres are tested.

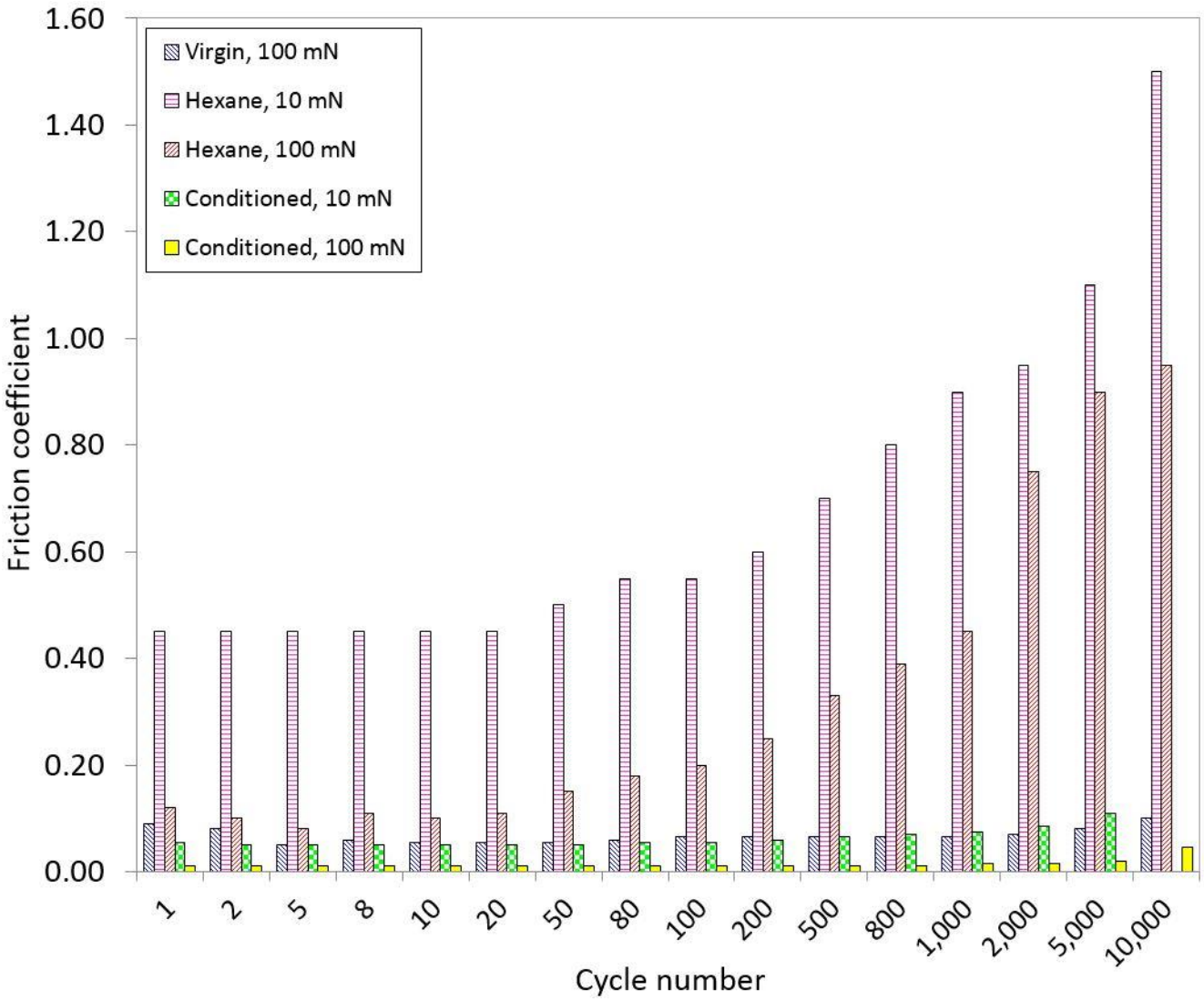

Figure 10. Tribological testing results for all hair fibres. The coefficient of friction is displayed as a function of cycle number.

5. Conclusion

An experimental study of the tribological properties of hair fibres has been performed, in which the effect of surface treatment on the evolution of friction and wear during sliding is considered. Orthogonally crossed fibre/fibre contacts held under a compressive normal load were investigated using constant velocity sliding. Studies were performed for 10,000 cycles, followed by interferometric imaging of the region of the hair fibre that had been exposed to tribological testing. Scanning electron microscopy was found to be useful for rapid qualitative inspection of fibres, affording identification of target regions in preparation for interferometric imaging, which yielded quantitative roughness information. Hair fibres which presented sebum or conditioned product at the fibre/fibre junction exhibited smaller coefficient of frictions than hexane cleaned hair fibres. The values were also observed to depend on the directionality of sliding. Cuticle flattening was observed for fibre/fibre contacts exposed to 10 mN compressive normal loads, whereas loads of 100 mN introduced substantial cuticle wear and fibre damage.

The methodology presented here provides a valuable tool for studying the tribological properties of fibre/fibre contacts in greater detail, and for a wider range of experimental conditions considered in this work. Extending the methodology such that multiple tests can be performed simultaneously would be of great benefit to both academia and industry. Furthermore, the technique could be extended beyond the personal care industry to other fields that have interests in micron-scale fibres and their wear, for example the investigation of fibre optic cables, or single metal fibres used in microelectronics and microelectromechanical systems.

Conflict of interest

The authors declare no competing financial interest.

Author Contributions

The manuscript was written through contributions of all authors. All authors have given approval to the final version of the manuscript.

Funding sources

This work was funded by Unilever R&D Port Sunlight.

Acknowledgment

The Interferometer and Nanotribometer used in this research was obtained, through Birmingham Science City: Innovative Uses for Advanced Materials in the Modern World (West Midlands Centre for Advanced Materials Project 2), with support from Advantage West Midlands (AWM) and partly funded by the European Regional Development Fund (ERDF).

References

1. Neufeld, A.H.; Conroy, G.C.; *Evol. Anthropol.*, **2004**, *13*, 89.
2. Swift, J.A., in Van Neste, D.J.J. and Randall, V.A. (Eds), Hair Research For The Next Millenium, *Elsevier*, **1996**, 109-112.
3. Swift, J.A.; Smith, J.R.; *Scanning*, **2000**, *22*, 310-318.
4. Swift, J.A.; *J. Soc. Cosmet. Chem.*, **1997**, *48*, 123-126.
5. Swift, J.A.; *Int. J. Cosmet. Sci.*, **1999**, *21*, 227-239.
6. Swift, J.A.; *J. Cosmet. Sci.*, **1999**, *50*, 23-47.
7. Swift, J.A.; Smith, J.R.; *J. Microsc.*, **2001**, *204*, 203-211.
8. Bhushan, B.; Wei, G.; Haddad, P.; *Wear*, **2005**, *259*, 1012-1021.
9. LaTorre, C.; Bhushan, B.; *Ultramicroscopy*, **2005**, *105*, 155-175.
10. Wei, G.; Bhushan, B.; Torgerson, P.M.; *Ultramicroscopy*, **2005**, *105*, 248-266.
11. Wei, G.; Bhushan, B.; *Ultramicroscopy*, **2006**, *106*, 742-754.
12. Seshadri, I.P.; Bhushan, B.; *Acta Mater.*, **2008**, *56*, 774-781.
13. Breakspear, S; Smith, J.R.; Luengo, G.; *J. Struct. Biol.*, **2005**, *149*, 235-242.
14. Chen, N.; Bhushan, B.; *J. Microsc.*, **2005**, *220*, 96-112.
15. Chen, N.; Bhushan, B.; *J. Microsc.*, **2005**, *221*, 203-215.
16. LaTorre, C.; Bhushan, B.; *J. Vac. Sci. Technol. A*, **2005**, *23*, 1034-1045.
17. LaTorre, C.; Bhushan, B.; *J. Cosmet. Sci.*, **2006**, *57*, 37-56.
18. LaTorre, C.; Bhushan, B.; *Ultramicroscopy*, **2006**, *106*, 720-734.
19. Bhushan, B.; *Prog. Mater. Sci.*, **2008**, *53*, 585-710.
20. Max, E.; Häfner, W.; Bartels, F.W.; Sugiharto, A.; Wood, C.; Fery, A.; *Ultramicroscopy*, **2010**, *110*, 320-324.
21. Mizuno, H.; Luengo, G.S.; Rutland, M.W.; *Langmuir*, **2010**, *26*, 18909-18915.
22. Nikogeorgos, N.; Fletcher, I.W.; Boardman, C.; Doyle, P.; Ortuoste, N.; Leggett, G.J.; *Biointerphases*, **2010**, *5*, 60-68.
23. Mate, C.M.; Tribology On The Small Scale, *Oxford University Press (Oxford)*, **2008**.
24. Adams, M.J.; Briscoe, B.J.; Wee, T.K.; *J. Phys. D Appl. Phys.*, **1990**, *23*, 406-414.
25. Mizuno, H.; Luengo, G.S.; Rutland, M.W.; *Langmuir*, **2013**, *29*, 5857-5862.
26. Johnson, K.L.; Contact Mechanics, *Cambridge University Press (Cambridge)*, **1985**.
27. Bhushan, B.; Biophysics Of Human Hair, *Springer (Berlin)*, **2010**.
28. Hu, Z.; Xie, H.; Hua, T.; Wang, Z.; *Rev. Sci. Instrum.*, **2009**, *80*, 013105.
29. Lee, J.; Kwon, H.J.; *Int. J. Cosmetic Sci.*, **2013**, *35*, 238-243.

Appendix

A1. Contact radius for two orthogonally crossed hair fibres

According to Hertzian theory of contact mechanics, the radius, a, of the contact spot formed upon contact of two orthogonally crossed cylinders is given by:

$$a = \left(\frac{3PR}{4E^*}\right)^{\frac{1}{3}} \quad \text{(A1-1)}$$

where, P is the compressive normal load, R is the effective radius, given by Eq. A1-2, and E^* is the effective modulus, given by Eq. A1-3:

$$\frac{1}{R} = \frac{1}{R_1} + \frac{1}{R_2} \quad \text{(A1-2)}$$

$$\frac{1}{E^*} = \frac{1-\nu_1^2}{E_1} + \frac{1-\nu_2^2}{E_2} \quad \text{(A1-3)}$$

The maximum contact pressure, p_{max}, is given by:

$$p_{max} = \frac{3P}{2\pi a^2} \quad \text{(A1-4)}$$

For cylinder 1, $E_1 =$ Young's modulus, $R_1 =$ radius, $\nu_1 =$ Poisson's ratio. For cylinder 2, $E_2 =$ Young's modulus, $R_2 =$ radius, $\nu_2 =$ Poisson's ratio.

Assuming $E_1 = E_2 = 8$ GPa, $\nu_1 = \nu_2 = 0.38$, $R_1 = R_2 = 40$ µm, and $P = 100$ mN, then $a = 8.6$ µm, and $p_{max} = 642$ MPa.